

(This is a sample cover image for this issue. The actual cover is not yet available at this time.)

This article appeared in a journal published by Elsevier. The attached copy is furnished to the author for internal non-commercial research and education use, including for instruction at the authors institution and sharing with colleagues.

Other uses, including reproduction and distribution, or selling or licensing copies, or posting to personal, institutional or third party websites are prohibited.

In most cases authors are permitted to post their version of the article (e.g. in Word or Tex form) to their personal website or institutional repository. Authors requiring further information regarding Elsevier's archiving and manuscript policies are encouraged to visit:

<http://www.elsevier.com/copyright>



Contents lists available at SciVerse ScienceDirect

Bioresource Technology

journal homepage: www.elsevier.com/locate/biortech

Methylene blue adsorption onto swede rape straw (*Brassica napus* L.) modified by tartaric acid: Equilibrium, kinetic and adsorption mechanisms

Yanfang Feng^a, Hui Zhou^a, Guohua Liu^b, Jun Qiao^a, Jinhua Wang^a, Haiying Lu^a, Linzhang Yang^{a,c,*}, Yonghong Wu^{a,*}

^aState Key Laboratory of Soil and Sustainable Agriculture, Institute of Soil Science, Chinese Academy of Sciences, No. 71 East Beijing Rd., Nanjing 210008, PR China

^bBamboo Research Institute, Nanjing Forestry University, No. 159 Longpan Rd., Nanjing 210037, PR China

^cJiangsu Academy of Agriculture Sciences, No. 50 Zhongling Rd., Nanjing 210014, PR China

H I G H L I G H T S

- ▶ Swede rape straw modified by tartaric acid (SRSTA) is an efficient dye adsorbent.
- ▶ It is the first time to modify swede rape straw into bioadsorbent to remove dye.
- ▶ The dye adsorption capacity of SRSTA is high, competitive to activated carbon.
- ▶ The adsorption mechanism and kinetics were systematically investigated.

A R T I C L E I N F O

Article history:

Received 30 May 2012

Received in revised form 27 August 2012

Accepted 28 August 2012

Available online 7 September 2012

Keywords:

Methylene blue

Tartaric acid

Swede rape straw (*Brassica napus* L.)

Adsorption

Bioadsorbent

A B S T R A C T

The aim of this study was to develop a promising and competitive bioadsorbent with the abundant of source, low price and environmentally friendly characters to remove cationic dye from wastewater. The swede rape straw (*Brassica napus* L.) modified by tartaric acid (SRSTA) was prepared, characterized and used to remove methylene blue (MB) from aqueous solution at varied operational conditions (including MB initial concentrations, adsorbent dose, etc.). Results demonstrated that the equilibrium data was well fitted by Langmuir isotherm model. The maximum MB adsorption capacity of SRSTA was 246.4 mg g⁻¹, which was comparable to the results of some previous studied activated carbons. The higher dye adsorption capacity could be attributed to the presence of more functional groups such as carboxyl group on the surface of SRSTA. The adsorption mechanism was also discussed. The results indicate that SRSTA is a promising and valuable adsorbent to remove methylene blue from wastewater.

© 2012 Elsevier Ltd. All rights reserved.

1. Introduction

Every year, millions of tons of highly colored wastewater are discharged from different sources including plastic, textile, leather, cosmetics, paper-making, printing and dye manufacturing industries (Feng et al., 2011; Liu et al., 2012). It is very important to treat the colored synthetic compounds as they are hazardous to human being and environments. Methylene blue is one of the most important synthetic dyes that can negatively affect photosynthesis (Vargas et al., 2012). Many techniques, such as adsorption, coagulation, flocculation, oxidation, etc., have been developed to remove synthetic dyes from aqueous solutions (Somasekhara Reddy et al., 2012; Yu et al., 2012). Adsorption technology is one of the widely used treatment technologies to remove synthetic dyes from waste-

water because of the negligible one-time investment, separation-easy and use-conveniently (Asgher and Bhatti, 2012).

Although activated carbon (AC) is regarded as the highest efficient adsorbent, it is too expensive to be employed in purifying dye-contaminated wastewater, especially in large scale waters (Chatterjee et al., 2011). Consequently, various low-cost adsorbents, such as crude biomass, chemically modified biomaterials and some industrial wastes were investigated in order to provide a competitive substitute for ACs in purifying the colored wastewater (Mahmoud et al., 2012; Piccin et al., 2012). But these low-cost adsorbents (e.g., crude biomaterials) were either inefficient in adsorption capacity (Zhou et al., 2011) or may cause more serious damage to the environment during the production (e.g., most chemical modified adsorbents) (Dawood and Sen, 2012; Rivera-Utrilla et al., 2011). Thereafter, to improve the adsorption capacity of crude bioadsorbents such as various agro-based straws and to lower the negative effects (such as HCl, NaOH, H₂SO₄, etc.) during the development of bioadsorbents, tartaric acid (TA), a carboxylic

* Corresponding authors. Address: 71, East Beijing Rd., Nanjing, Jiangsu 210008, PR China. Tel./fax: +86 25 86881591.

E-mail addresses: lzyang@issas.ac.cn (L. Yang), yhwu@issas.ac.cn (Y. Wu).

Nomenclature

C_0	initial MB concentration (mg L^{-1})	$q_{e,\text{cal}}$	the amount of dye adsorbed onto the adsorbents calculated by model at equilibrium (mg g^{-1})
C_e	MB concentration at equilibrium (mg L^{-1})	q_t	the amount of dye adsorbed onto the adsorbents at time t (mg g^{-1})
C_t	MB concentration at time t (mg L^{-1})	q_m	the maximum adsorption capacity for adsorbent (mg g^{-1})
C	Intra-particle diffusion model constant	$q_{m,\text{cal}}$	the maximum adsorption capacity calculated by mathematic model (mg g^{-1})
B_t	Boyd model constant	R	ideal gas constant ($8.314 \text{ J mol}^{-1} \text{ K}^{-1}$)
k_1	pseudo-first-order kinetic model rate constant (min^{-1})	R^2	correlation coefficient
k_2	pseudo-second-order kinetic model rate constant ($\text{g mg}^{-1} \text{ min}^{-1}$)	t	time (min)
K_L	Langmuir adsorption constant (L mg^{-1})	V	the volume of solutions (L)
K_F	Freundlich adsorption constant (mg g^{-1})		
k_{id}	intraparticle rate constant ($\text{mg g}^{-1} \text{ min}^{-0.5}$)		
m	mass of adsorbent (g)		
n	Freundlich constant		
q_e	the amount of dye adsorbed onto the adsorbents at equilibrium (mg g^{-1})		

acid with mild chemical properties, inexpensive and environmentally friendly profile was applied to modify swede rape straw (*Brassica napus* L.). Swede rape straw is a widespread and promising agro-based biomass. As one of the most important edible oils, a large amount of rapeseed oil, which was estimated about 21.39 million metric tons, is produced annually (Zhang et al., 2010). Consequently, the amount of rape straw would be much larger and could effectively be used as an adsorbent to treat the wastewater.

Considering the above facts, the main objectives of this study were to (1) develop and characterize the swede rape straw modified by tartaric acid (SRSTA); (2) investigate the effects of various operational conditions including particle size, TA concentration, adsorbent dose, solution initial dye concentrations, etc., on adsorption processes during the development of SRSTA and the removal of methylene blue; (3) describe the adsorption process using mathematical models and (4) discuss the adsorption mechanism of methylene blue onto SRSTA. Different crude bioadsorbents have been used to treat the wastewater, but to the best of our knowledge, this is the first report on developing and applying chemical (TA) modified swede rape straw (*Brassica napus* L.) to purify dye-contaminated wastewater. The finding will provide a promising biomeasure to remove methylene blue, and also give insight to explain the process of SRSTA adsorbing methylene blue and similar synthetic hazardous compounds.

2. Methods

2.1. Adsorbent and adsorbate

The crude swede rape straw (dry) was collected from Suzhou Academy of Agriculture Sciences, PR China. The straw was cut to small pieces (length about 0.5 cm), washed with deionized water and dried at 60 °C. Then the dried biomass was crushed, sieved (250 μm) and activated at 110 °C for 2 h, which was designated as SRS. The producing process of SRSTA is presented by Fig. 1. Finally, the prepared SRSTA was stored in a brown reagent bottle for the following experiments.

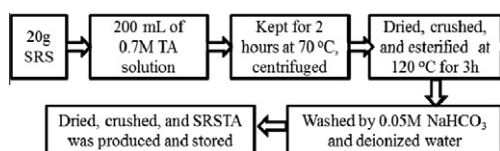


Fig. 1. The schematic diagram of the producing procedure of SRSTA.

Methylene blue ($\text{C}_{16}\text{H}_{18}\text{ClN}_3\text{S}_3\text{H}_2\text{O}$, FW = 373.9, C.I.52015, $\lambda_{\text{max}} = 664 \text{ nm}$) was used as a model dye to test the adsorption capacity and to investigate the adsorption process. This cationic dye was purchased from Sinopharm Chemical Reagent Co. LTD (Shanghai, China). All other chemicals used were of analytical grade.

2.2. Adsorption experiment

The concentration of the MB stock solution for adsorption experiment was 1000 mg L^{-1} . The pH of the solution was adjusted to 8.0. The concentration of MB was measured according to the following process (Feng et al., 2011). Briefly, approximately 5 mL of MB solution was filtered through 0.45 μm membrane filters (the first 2 mL solution was discarded), diluted to appropriate concentrations to make sure that their absorbance remained within the linear calibration range and then measured at 664 nm using a UV-vis spectrophotometer (Shimadzu, UV2450, Japan). Measurements of MB concentrations were reproducible within 10%. The amount of MB adsorbed onto bioadsorbents at equilibrium and at time t was obtained by means of the following equations:

$$q_e = \frac{(C_0 - C_e)V}{m} \quad (1)$$

$$q_t = \frac{(C_0 - C_t)V}{m} \quad (2)$$

The bioadsorbents were characterized by SEM scanning (Quanta 200, FEI, Netherlands) at a magnification of 500 \times and 1600 \times , respectively; FTIR scanning (Nicolet 360, Thermo Electron Co., USA) at a spectral range of 4000–400 cm^{-1} ; XRD study with the 2θ angle ranged from 0° to 70° (D/max - $^\circ\text{C}$, Rigaku Corporation, Japan); TGA-DTG study with the temperature from 30 to 700 °C (Pyris 1 TGA, PerkinElmer, USA) and particle size distribution analyzing (Mastersizer 2000, Malvern Instruments, UK).

Each experiment was repeated three times and the mean results with error bar ($\pm\text{SD}$) were presented. All figures (if necessary) were derived using Origin 8.0.

2.3. Theory

Isotherms study is important for developing a model that can be used for adsorption process design (Li et al., 2011). Two widely used equilibrium isotherm models, i.e., Langmuir model and Freundlich model, were applied to describe the adsorption. The detailed information about these two models were presented in the former manuscript (Feng et al., 2011).

To evaluate the adsorption process, two kinetic models were used:

Pseudo-first-order kinetic model.

$$\log(q_e - q_t) = \log q_e - \frac{k_1}{2.303} t \quad (3)$$

Ho's pseudo-second-order kinetic model (Ho, 2003).

$$\frac{t}{q_t} = \frac{1}{k_2 q_e^2} + \frac{t}{q_e} \quad (4)$$

Intra-particle diffusion model is useful to identify the adsorption mechanism that can be expressed by the following equation:

$$q_t = k_{id} t^{0.5} + C \quad (5)$$

Meanwhile, Boyd's model was applied to predict the actual slow step involved in the adsorption process, and it is expressed as follows (Tang et al., 2012):

$$B_t = -0.4977 - \ln\left(1 - \frac{q_t}{q_e}\right) \quad (6)$$

3. Results and discussion

3.1. Characterization of bioadsorbent

3.1.1. The morphology of the bioadsorbent

Scanning electron microscope (SEM, see Fig. 1S in S.I.) was used to analyze the surface morphology of crude SRS and MB-loaded SRSTA (SRSTA-MB). Crude SRS contained a rough surface with regular tunnel-like structure (Fig. 1S-a), in addition, many tiny pores were observed on the surface of the tunnel-like structure (Fig. 1S-b). These structures, which were due to the remains of dried cell wall, would provide a comparatively large surface area. After TA modification (Fig. 1S-c), no significant variations were found between SRS and SRSTA. It implies that the chemical modification did not damage the well-developed porous structure. Further, the SEM image of dye-loaded SRSTA (SRSTA-MB, Fig. 1S-d) showed an obviously changed surface morphology: the surface became much smoother than that of the previous image. The results indicated that large amount of MB may be attached on the surface of SRSTA.

3.1.2. Responsible functional groups

FTIR spectra are useful to identify the functional groups associated with the surface of bioadsorbents and the functional groups involved in the adsorption process could also be identified (Khan et al., 2011). To investigate the responsible functional groups, the FTIR spectra of the two relevant biomaterials (i.e., SRS and SRSTA) were studied (Fig. 2S). The obviously changed peaks and the possible reasons have been listed in Table 1. The changes of main peaks between SRS and SRSTA were occurred around 1739.16 and 1044.41 cm^{-1} . The two peaks of SRSTA were much higher and sharper than these of SRS. It showed that carboxyl group ($-\text{COO}^-$) increased prominently after the TA modification.

3.1.3. The changes in crystalline structures

Chemical modification process may lead to some changes in the crystalline structure of the biomaterials (Khan et al., 2011). Thus, X-ray diffraction (XRD) study was conducted to investigate the possible changes in the crystalline structures of SRS and SRSTA. The XRD pattern of raw SRS showed typical spectrum of cellulosic materials (Fig. 3S). The largest peak (at around 22°) indicated the presence of highly organized crystalline cellulose, while the smaller peak (at around 16°) indicated a less organized polysaccharide structure (Gong et al., 2005). The increased peak height after TA

Table 1

The main peak changes in FTIR spectra of bioadsorbents before and after TA modification.

Peaks (wave numbers)	Vibrations or stretching of functional groups
3429.17	O–H bond stretching vibrations
2921.86	C–H in the aliphatic hydrocarbons
1739.16	Absorption peak of C=O bond
1628.40	Absorption peak of aromatic ring
1502.93	C=C bond (aromatic ring)
1044.41	Absorption peak of C=O bond
884.08	Absorption peak of methyl group

modification indicated the increased crystallinity. It is noteworthy that, after TA modification no new peak in the spectra of SRSTA was appeared. This result indicated that TA modification did not generate crystals on the surface of bioadsorbents.

3.1.4. Thermogravimetric analysis

Thermogravimetric analysis of SRS and SRSTA was conducted to understand the thermal characteristics and weight loss of the both bioadsorbents. Results shown in Fig. 2a demonstrated that both biomaterials were pyrolysed below 500°C , and the remained ash accounted for 9–11% of the biomaterials. A small loss of mass is observed at temperatures below 100°C , which can be attributed to the loss of water (Avelar et al., 2010). Moreover, a major peak was appeared at around $300\text{--}350^\circ\text{C}$ (shown in DTG curves). This could be attributed to the decomposition of some compounds that exists in most biomass, such as lignin, cellulose, hemicelluloses, etc. (Gao et al., 2008). It should be noted that there was a minor peak at around $260\text{--}270^\circ\text{C}$ for SRSTA while there was no such peak in case of crude biomaterial SRS. It has been recognized that TA decomposed at around 210°C , which proved that the minor peak was not due to the decomposition of TA crystal that may exist after TA modification. Results of FTIR study showed that many esterified groups were emerged after TA modification. The minor peak of SRSTA may be due to the presence of the newly emerged ester compounds. In addition, the DTG curve showed no TA crystal on the surface of SRSTA, indicating that TA molecules were successfully reacted with the surface functional groups (i.e., $-\text{OH}$ group) on SRS.

3.2. Operational conditions and environmental effects on adsorption

3.2.1. Effect of particle size and TA concentration on adsorption capacity

Due to the extra grinding process during the production of SRSTA, there is a possibility to change the distribution of the particle size, which may finally affect the adsorption capacity of the bioadsorbents. In order to investigate the effects caused by the variation of particle size, and to prove that the improvement of dye adsorption capacity of SRSTA was dominated by TA modification instead of the variation of particle size, following experiments were conducted.

Firstly, the variation of particle size was examined by a particle size analyzer (Fig. 2b), which proved that the particle size of SRSTA was smaller than that of SRS (volume mean diameter decreased from 204.9 to 103.4 μm for SRS and SRSTA, respectively). Smaller particle size indicated larger specific surface area, which consequently lead to more adsorption site and higher adsorption capacity.

Secondly, to investigate the effect of the particle size on adsorption capacity, SRS with four different particle size distributions were used to adsorb MB from aqueous solutions (Fig. 2c). Fig. 2c showed that the q_e values merely increased about 6% when the particle size of SRS decreased from 100–150 to 0–100 μm . This

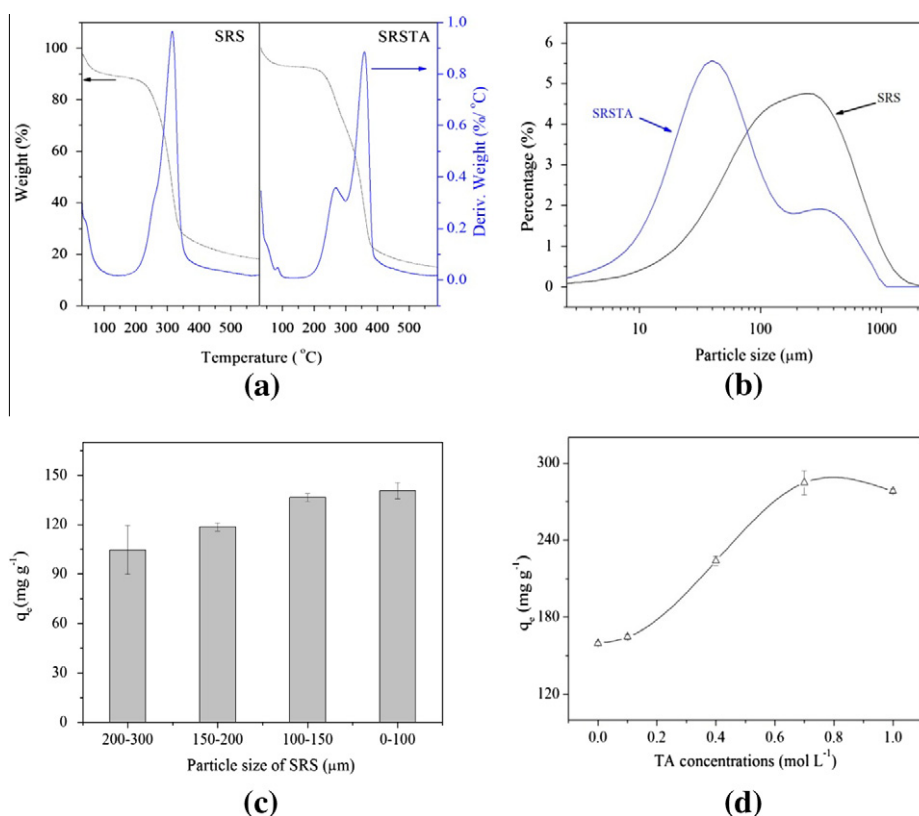


Fig. 2. (a) TGA-DTG curves of SRS and SRSTA (30 to 700 °C); (b) Particle size distribution of SRS and SRSTA; (c) The adsorption capacity of MB by SRS with different particle size distribution (experiment conditions: initial MB concentration = 500 mg L⁻¹, sorbent dose = 1 g L⁻¹, pH = 8.0); (d) The effect of different TA concentrations on the adsorption capacity of SRSTA (adsorption experiment conditions: initial MB concentration = 500 mg L⁻¹, sorbent dose = 1 g L⁻¹, pH = 8.0).

observation is consistent with some previous studies (Asgher and Bhatti, 2012): the adsorption capacity of bioadsorbents usually reaches a plateau under a certain range of particle size distributions.

Furthermore, the q_e values of SRSTA modified by different concentrations of TA solutions were tested. The crude SRS was prepared under the same operational conditions before chemical modification. Consequently, the variation of q_e values in this experiment was dominated by TA concentrations. Results indicated increased q_e values when TA concentrations were lower than 0.7 M (Fig. 2d), whereas q_e values did not change to a larger extent at higher (≥ 0.7 M) TA concentrations. This result directly proved that the increase of MB adsorption capacity was dominated by TA concentrations instead of particle size distributions. Results of this study demonstrated that 0.7 M TA concentrations should be selected under the present experimental conditions to produce an efficient SRSTA with the lowest TA consumption (Fig. 2d).

In conclusion, particle size slightly affects the adsorption capacity of relevant bioadsorbents, whereas TA concentrations largely influence the adsorption capacity. Thus the increase of dye adsorption capacity of SRSTA was dominated by TA modification instead of the changes of particle size distribution.

3.2.2. Effect of dose on adsorption

Fig. 3a shows the effect of SRSTA dose on MB adsorption. Results of the study indicated that with the increased adsorbent doses the q_e values decreased while the removal percentage of dye increased. When the adsorbent dose increase, the number of sorption sites on the surface of adsorbents will increase, this will enlarge the concentration gradient between the dye concentration in the solution and the dye concentration in the surface of the bioadsorbents (Dawood and Sen, 2012). The enlarged concentration gradient will

enhance the interaction between MB molecules and adsorbent (SRSTA), which will consequently improve the removal percentage of MB. In addition, the total amount of MB molecules is the same for a certain volume of MB solution, for every adsorption site, the increased amount of adsorbents for the solutions will lower the driving force and lead to a lower q_e values.

3.2.3. Effect of sampling time and initial MB concentration on adsorption

In order to investigate the effect of adsorption time and dye concentrations on the adsorption process, two initial MB concentrations (200 and 400 mg L⁻¹) were selected and sampled at different time intervals. According to Fig. 3b, q_t values for both MB concentrations were increased with the increased sampling time before reaching the equilibrium (within 40–60 min). Higher q_t values were observed in higher initial dye concentration (400 mg L⁻¹), than that of the lower dye concentrations (200 mg L⁻¹). While, the removal percentages were lower in higher initial MB concentrations as compared to the lower initial MB concentrations (data not shown). Dye concentration provides an important driving force to overcome the mass transfer resistance between bioadsorbents and aqueous solutions. It means that at higher initial dye concentrations, the driving force was higher than that of the lower initial dye concentrations. Consequently, the q_t values would be higher in case of higher initial dye concentrations. However, at higher initial dye concentrations the available sorption sites becomes comparatively fewer, and hence lowering the removal percentage of MB.

Moreover, time needed to attain the equilibrium is obviously different for different initial dye concentrations. According to Fig. 3b, time needed to reach equilibrium was longer for the initial dye concentration of 400 mg L⁻¹ (about 60 min) than that of the dye concentration of 200 mg L⁻¹ (around 40 min). That happens

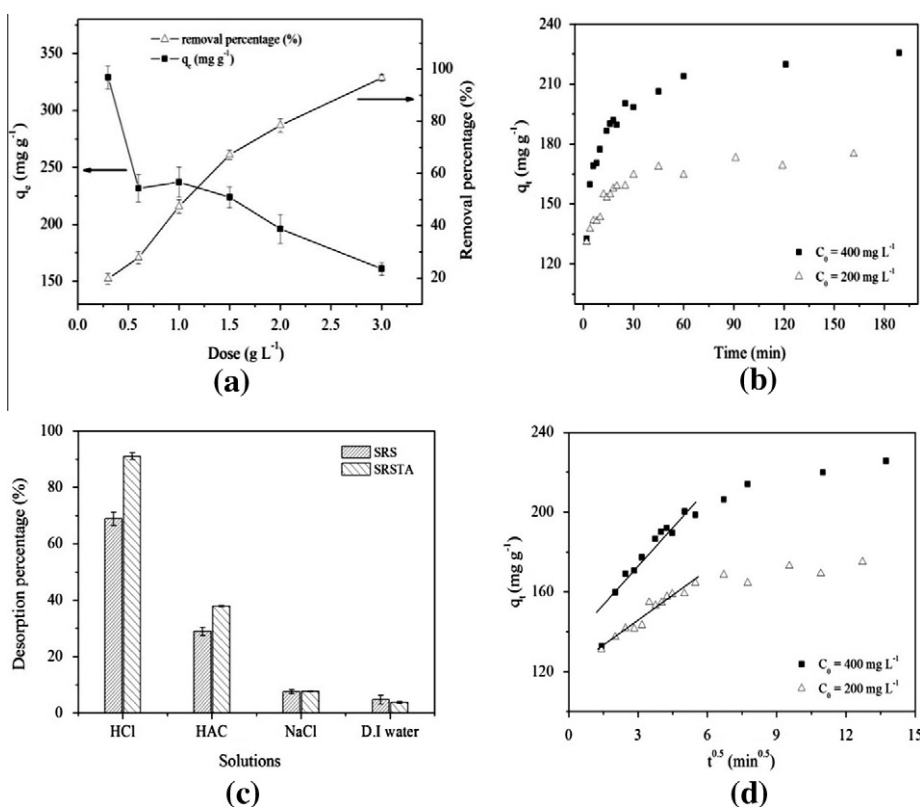


Fig. 3. (a) The effect of SRSTA dose on the adsorption capacity and dye removal percentages (experiment conditions: initial MB concentration = 500 mg L⁻¹, pH = 8.0); (b) The effect of time and initial MB concentrations on adsorption (experiment conditions: sorbent dose = 1 g L⁻¹, pH = 8.0, sampling time from 2 min to about 180 min, with different time intervals); (c) Desorption study with different solutions (experiment conditions: solute concentrations = 0.01 mol L⁻¹); (d) Intraparticle diffusion study.

Table 2
Equilibrium parameters for Langmuir and Freundlich model, respectively.

Adsorbents	Langmuir			Freundlich		
	$q_{m,cal}$ (mg g ⁻¹)	K_L (L mg ⁻¹)	R^2	n	K_F (mg g ⁻¹)	R^2
SRSTA	246.4	0.1160	0.9916	4.985	88.85	0.9778
SRS	128.2	0.0968	0.9987	6.636	55.60	0.8822

because, at higher initial dye concentrations, the sorption sites on the surface of bioadsorbents were not sufficient to attach most of the MB molecules in the aqueous solutions and part of the unattached molecules needs to penetrate the boundary layer on the surface and enter into the bioadsorbent particles through intraparticle diffusion. Consequently, the time needed to reach equilibrium was longer at higher initial dye concentrations because of the time-consuming intraparticle diffusion process (i.e., rate-limiting step). This result was similar to many previous studies (Kyzas et al., 2012; Mahmoud et al., 2012; Somasekhara Reddy et al., 2012).

3.3. Adsorption process and mechanisms

3.3.1. Equilibrium study

Equilibrium study is important as it provides the qualitative information on the nature of solute-solid surface interactions and could be used to evaluate the adsorption capacity of a particular adsorbent. In this study, two widely used isotherm models, i.e., Langmuir model and Freundlich model were used to describe the adsorption process. The relevant parameters of these models were given in Table 2 and the isotherm experiment plots together with curves were presented in Fig. 4S.

Obviously, Langmuir model fits to the experimental data in a better way (Table 2, $R^2 > 0.99$), which means the adsorption of

MB onto SRSTA/SRS occurred as a monolayer adsorption. According to the assumption of Langmuir model, the adsorption affinity on the surface of the SRSTA/SRS is homogenous in terms of surface functional groups and bonding energy, and the surface contains a finite number of identical adsorption sites (Dawood and Sen, 2012; Khambhaty et al., 2012). In addition, the calculated value for maximum amount of MB loaded on the bioadsorbents ($q_{m,cal}$) were given in Table 2. It showed that the $q_{m,cal}$ value of SRSTA was significantly higher (roughly 2 times higher) than that of the crude SRS. The adsorption capacity of SRSTA was higher than many previous studied bioadsorbents (Han et al., 2012; Liu et al., 2012; Mahmoud et al., 2012; Sen et al., 2011; Song et al., 2011; Vieira et al., 2012) and even competitive compared with some lab-produced or commercial activated carbons (Avelar et al., 2010; Girgis et al., 2011; Mahmoud et al., 2012; Raposo et al., 2009). SRSTA is very competitive due to its higher adsorption capacity for cationic dyes, ideal environment-friendly profile and low-cost involved to produce from agro-based biomass. All of these characteristics will make SRSTA a feasible low-cost substitute for ACs in purifying dye-contaminated waste water through adsorption technology.

Compared with Langmuir model, the determined correlation coefficient (R^2) of Freundlich model was lower for both bioadsorbents. The Freundlich isotherm model assumes a multilayer adsorption that occurred on a heterogeneous surface, and the heat

Table 3

Parameters of pseudo-second-order kinetic model, pseudo-first-order kinetic model and intraparticle diffusion model at different initial dye concentrations.

C_0 (mg L ⁻¹)	Pseudo-second-order kinetic model		Pseudo-first-order kinetic model			Intraparticle diffusion model		
	$q_{e,cal}$ (mg g ⁻¹)	k_2 (g mg ⁻¹ min ⁻¹)	R^2	k_1 (min ⁻¹)	R^2	k_{id} (mg g ⁻¹ min ^{-0.5})	C (mg g ⁻¹)	R^2
200	172.4	0.003797	0.9995	0.00397	0.7295	11.76	120.5	0.9487
400	223.2	0.001718	0.9994	0.02174	0.8898	8.31	139.4	0.9431

of adsorption is not uniform between the molecules that adsorbed onto the adsorbent surface. The Freundlich isotherm model did not fit well with the experimental data indicating its inapplicability to describe these isotherm data.

3.3.2. Kinetic study

Kinetic study is necessary because it presents critical parameters (e.g., present the adsorption rate, predicting the q_e values, etc.) in designing an industrial adsorption column. In the present study, two widely used kinetic models, i.e., pseudo-first-order and Ho's pseudo-second-order kinetic model are selected to characterize the adsorption process of SRSTA under two different initial dye concentrations. The plots corresponding to the regression curves were presented in Figs. 5S-a and 5S-b. Meanwhile, the relevant parameters were shown in Table 3. According to Table 3, the regression correlation coefficients (R^2) of pseudo-second-order kinetic model were significantly higher than that of the pseudo-first-order kinetic model. This result indicated that the adsorption of MB onto SRSTA obeys pseudo-second-order kinetic model very well, which is similar to many previous studies (Feng et al., 2011; Mahmoud et al., 2012). Considering the inapplicability of pseudo-first-order kinetic model presented in Table 3, it will not be discussed in detail here.

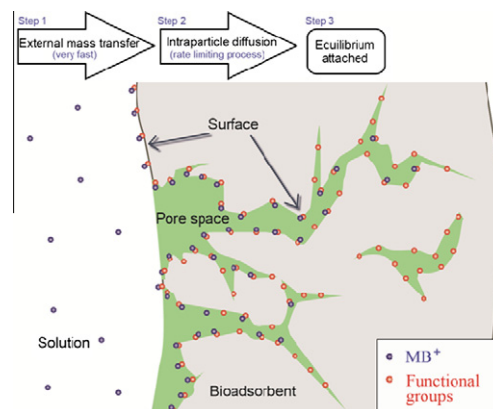
It is obvious from Table 3 that the $q_{e,cal}$ values were very close to the experimental q_e values, increased with the increasing of initial dye concentrations; but the rate constants (k_2 values) decreased with the increasing of C_0 . At higher MB concentrations, the competition for the surface sorption sites will be high, which will consequently lead to a comparatively low rate constant (Nethaji and Sivasamy, 2011).

3.3.3. Desorption study

Desorption study is usually applied to elucidate the adsorption mechanism and to recover the depleted adsorbent (Yu et al., 2011). In this study, four solutions were used: hydrochloric acid solution, acetic acid solution, sodium chloride solution and deionized water. To compare the efficiency of different solutions in desorption study, the concentration of solutes were set as 0.01 M (except the deionized water). If the attached dye molecule desorbed by deionized water, the adsorption is usually dominated by weak bonds; otherwise, if it is desorbed by acid, the adsorption is dominated by ion exchange (Chen et al., 2011). According to Fig. 3c, hydrochloric acid solution is the most efficient one (91.01% for SRSTA), following acetic acid solution. Sodium chloride solution and deionized water were inefficient to desorb MB molecules in the present study. It implies that ion change was the dominating mechanism in adsorbing MB onto both bioadsorbents.

3.3.4. Adsorption mechanisms

For a solid–liquid adsorption system, the solute transfer is usually characterized by boundary layer diffusion, intra-particle diffusion or both, and the controlling step of the adsorption could be intraparticle and/or external diffusion process (Dawood and Sen, 2012). In order to understand the adsorption mechanism involved in the adsorption of MB onto SRSTA, the kinetic data were analyzed by intraparticle diffusion model Eq. (5) and Boyd's model Eq. (6).

**Fig. 4.** The schematic diagram of the adsorption process and mechanism.

According to the result shown in Fig. 3d, the adsorption process could be divided into three steps (Feng et al., 2011). The first step that completed within about 2 min was dominated by external mass transfer. Because of the existence of some functional groups on the external surface of SRSTA (especially $-\text{COO}^-$ groups that confirmed by FTIR spectra in Fig. 2S), the rapid attachment was probably due to the strong electrostatic attraction between MB^+ and $-\text{COO}^-$. Thereafter, the second step that finished within about 40 min could be attributed to the intraparticle diffusion process. The sorption sites were not sufficient to attach most of the MB molecules after the first rapid stage (electrostatic attraction), the concentration gradient between the solution and the solid inner surface (i.e., pores or caves) is still large enough to drive the adsorption. However, this process was the rate-limiting step and at least 40 min were needed to finish this process under the present experiment conditions. The third step was the equilibrium stage. After a period of adsorption, the adsorbate concentration in the solutions was too low to drive the adsorption, i.e., the intraparticle diffusion starts to slow down and finally ceased, which indicated that equilibrium was attained. Based on the above analysis, a schematic diagram of the adsorption process and mechanism is shown in Fig. 4. Functional groups shown in this schematic diagram includes carboxyl group, hydroxyl group, etc.

The C value in Eq. (5) represents the boundary layer effect (film diffusion). Higher C values indicate greater contributions of the surface sorption in the rate-controlling step. According to Table 3, the C values were increased with the increase of initial dye concentrations, which indicates the increased boundary layer thickness at higher initial dye concentrations. Likewise, the k_{id} values were increased with the increasing dye concentrations. At higher initial dye concentrations, the adsorption driving force was stronger, consequently it will cause an enhanced MB diffusion rate (Weng et al., 2009). Furthermore, if the regression curves (Fig. 3d) for both initial dye concentrations are extended, they do not pass through the origin. It means some other mechanisms along with intraparticle diffusion are involved in the process (Özcan et al., 2005).

The boundary layer effect may control the rate of mass transfer in the slow-adsorption step, and it could be corroborated by the analysis of dynamic data from Boyd's model (Ahmad and Alrozi,

2011). If a plot of B_t versus t is a straight line and it passes through the origin (if extended), the adsorption will fit with the layer effect. According to Fig. 6S in S.I., the plots are linear only at the initial period ($0.8648 \leq R^2 \leq 0.8919$); meanwhile, the regression curve passes through the origin (approximately). It confirmed that at this period the rate-limiting process is to be governed by particle diffusion phenomena (Mittal et al., 2012).

4. Conclusion

The maximum monolayer adsorption capacity of SRSTA was calculated as 246.4 mg g^{-1} . The improvement of MB adsorption capacity after TA modification was mainly due to the increased functional groups on the surface of biomaterials. The adsorption process could be divided into three stages (external mass transfer, intraparticle diffusion and attach equilibrium). The intraparticle diffusion of MB molecules through the pores was the rate-limiting step. The present study indicates that tartaric acid modified swede rape straw (SRSTA) is an efficient, low-cost, environmental-friendly and easy-produced bioadsorbent and may be used as a promising bioadsorbent to remove the dye from industrial wastewater.

Acknowledgements

This work was supported by the National Specific Project for Water Pollution Control (2012ZX07101-004) and the National Key Technology R&D Program (2012BAJ24B06). The authors are grateful to Mr. Yun Tang from Southwest University of Science and Technology, China, for the helps of TGA-DTG analyze. The helps from Dr. M. M. Masud (ISSCAS) will also be appreciated.

Appendix A. Supplementary data

Supporting information (S.I.) associated with this article can be found, in the online version, at <http://dx.doi.org/10.1016/j.biortech.2012.08.128>.

References

- Ahmad, M.A., Alrozi, R., 2011. Removal of malachite green dye from aqueous solution using rambutan peel-based activated carbon: Equilibrium, kinetic and thermodynamic studies. *Chem. Eng. J.* 171 (2), 510–516.
- Asgher, M., Bhatti, H.N., 2012. Evaluation of thermodynamics and effect of chemical treatments on sorption potential of citrus waste biomass for removal of anionic dyes from aqueous solutions. *Ecol. Eng.* 38 (1), 79–85.
- Avelar, F.F., Bianchi, M.L., Gonçalves, M., da Mota, E.G., 2010. The use of piassava fibers (*Attalea funifera*) in the preparation of activated carbon. *Bioresource Technol.* 101 (12), 4639–4645.
- Chatterjee, S., Chatterjee, T., Lim, S.-R., Woo, S.H., 2011. Effect of the addition mode of carbon nanotubes for the production of chitosan hydrogel core-shell beads on adsorption of Congo red from aqueous solution. *Bioresource Technol.* 102 (6), 4402–4409.
- Chen, H., Zhao, J., Wu, J., Dai, G., 2011. Isotherm, thermodynamic, kinetics and adsorption mechanism studies of methyl orange by surfactant modified silkworm exuviae. *J. Hazard. Mater.* 192 (1), 246–254.
- Dawood, S., Sen, T.K., 2012. Removal of anionic dye Congo red from aqueous solution by raw pine and acid-treated pine cone powder as adsorbent: equilibrium, thermodynamic, kinetics, mechanism and process design. *Water Res.* 46 (6), 1933–1946.
- Feng, Y., Yang, F., Wang, Y., Ma, L., Wu, Y., Kerr, P.G., Yang, L., 2011. Basic dye adsorption onto an agro-based waste material – Sesame hull (*Sesamum indicum* L.). *Bioresource Technol.* 102 (22), 10280–10285.
- Gao, B., Peng, C., Chen, G.Z., Li Puma, G., 2008. Photo-electro-catalysis enhancement on carbon nanotubes/titanium dioxide (CNTs/TiO₂) composite prepared by a novel surfactant wrapping sol-gel method. *Appl. Catal. B: Environ.* 85 (1–2), 17–23.
- Girgis, B.S., Soliman, A.M., Fathy, N.A., 2011. Development of micro-mesoporous carbons from several seed hulls under varying conditions of activation. *Microporous Mesoporous Mater.* 142 (2–3), 518–525.
- Gong, R., Sun, Y., Chen, J., Liu, H., Yang, C., 2005. Effect of chemical modification on dye adsorption capacity of peanut hull. *Dyes Pigm.* 67 (3), 175–181.
- Han, X., Niu, X., Ma, X., 2012. Adsorption characteristics of methylene blue on poplar leaf in batch mode: equilibrium, kinetics and thermodynamics. *Korean J. Chem. Eng.* 29 (4), 494–502.
- Ho, Y.-S., 2003. Removal of copper ions from aqueous solution by tree fern. *Water Res.* 37 (10), 2323–2330.
- Khambhaty, Y., Mody, K., Basha, S., 2012. Efficient removal of Brilliant Blue G (BBG) from aqueous solutions by marine *Aspergillus wentii*: Kinetics, equilibrium and process design. *Ecol. Eng.* 41, 74–83.
- Khan, M.M.R., Ray, M., Guha, A.K., 2011. Mechanistic studies on the binding of Acid Yellow 99 on coir pith. *Bioresource Technol.* 102 (3), 2394–2399.
- Kyzas, G.Z., Lazaridis, N.K., Mitropoulos, A.C., 2012. Removal of dyes from aqueous solutions with untreated coffee residues as potential low-cost adsorbents: Equilibrium, reuse and thermodynamic approach. *Chem. Eng. J.* 189–190, 148–159.
- Li, Q., Yue, Q., Su, Y., Gao, B., 2011. Equilibrium and a two-stage batch adsorber design for reactive or disperse dye removal to minimize adsorbent amount. *Bioresource Technol.* 102 (9), 5290–5296.
- Liu, Y., Wang, J., Zheng, Y., Wang, A., 2012. Adsorption of methylene blue by kapok fiber treated by sodium chlorite optimized with response surface methodology. *Chem. Eng. J.* 184, 248–255.
- Mahmoud, D.K., Salleh, M.A.M., Karim, W.A.W.A., Idris, A., Abidin, Z.Z., 2012. Batch adsorption of basic dye using acid treated kenaf fibre char: equilibrium, kinetic and thermodynamic studies. *Chem. Eng. J.* 181–182, 449–457.
- Mittal, A., Thakur, V., Gajbe, V., 2012. Evaluation of adsorption characteristics of an anionic azo dye Brilliant Yellow onto hen feathers in aqueous solutions. *Environ. Sci. Pollut. R.*, 1–10.
- Nethaji, S., Sivasamy, A., 2011. Adsorptive removal of an acid dye by lignocellulosic waste biomass activated carbon: equilibrium and kinetic studies. *Chemosphere* 82 (10), 1367–1372.
- Özcan, A.S., Erdem, B., Özcan, A., 2005. Adsorption of Acid Blue 193 from aqueous solutions onto BTMA-bentonite. *Colloid Surf. A-Physicochem. Eng. Asp.* 266 (1–3), 73–81.
- Piccin, J.S., Gomes, C.S., Feris, L.A., Gutterres, M., 2012. Kinetics and isotherms of leather dye adsorption by tannery solid waste. *Chem. Eng. J.* 183, 30–38.
- Raposo, F., De La Rubia, M.A., Borja, R., 2009. Methylene blue number as useful indicator to evaluate the adsorptive capacity of granular activated carbon in batch mode: influence of adsorbate/adsorbent mass ratio and particle size. *J. Hazard. Mater.* 165 (1–3), 291–299.
- Rivera-Utrilla, J., Sánchez-Polo, M., Gómez-Serrano, V., Álvarez, P.M., Alvim-Ferraz, M.C.M., Dias, J.M., 2011. Activated carbon modifications to enhance its water treatment applications. An overview. *J. Hazard. Mater.* 187 (1–3), 1–23.
- Sen, T., Afroze, S., Ang, H., 2011. Equilibrium, kinetics and mechanism of removal of methylene blue from aqueous solution by adsorption onto pine cone biomass of *Pinus radiata*. *Water Air Soil Pollut.* 218 (1), 499–515.
- Somasekhara Reddy, M.C., Sivaramakrishna, L., Varada Reddy, A., 2012. The use of an agricultural waste material, Jujuba seeds for the removal of anionic dye (Congo red) from aqueous medium. *J. Hazard. Mater.* 203–204, 118–127.
- Song, J.Y., Zou, W.H., Bian, Y.Y., Su, F.Y., Han, R.P., 2011. Adsorption characteristics of methylene blue by peanut husk in batch and column modes. *Desalination* 265 (1–3), 119–125.
- Tang, H., Zhou, W., Zhang, L., 2012. Adsorption isotherms and kinetics studies of malachite green on chitin hydrogels. *J. Hazard. Mater.* 209–210, 218–225.
- Vargas, A.M.M., Cazetta, A.L., Martins, A.C., Moraes, J.C.G., Garcia, E.E., Gauze, G.F., Costa, W.F., Almeida, V.C., 2012. Kinetic and equilibrium studies: adsorption of food dyes Acid Yellow 6, Acid Yellow 23, and Acid Red 18 on activated carbon from flamboyant pods. *Chem. Eng. J.* 181–182, 243–250.
- Vieira, S.S., Magriotis, Z.M., Santos, N.A.V., Cardoso, M.D.G., Saczk, A.A., 2012. Macauba palm (*Acrocomia aculeata*) cake from biodiesel processing: an efficient and low cost substrate for the adsorption of dyes. *Chem. Eng. J.* 183, 152–161.
- Weng, C., Lin, Y., Tzeng, T., 2009. Removal of methylene blue from aqueous solution by adsorption onto pineapple leaf powder. *J. Hazard. Mater.* 170 (1), 417–424.
- Yu, X., Luo, T., Zhang, Y., Jia, Y., Zhu, B., Fu, X., Liu, J., Huang, X., 2011. Adsorption of lead(II) on O₂-plasma-oxidized multiwalled carbon nanotubes: thermodynamics, kinetics, and desorption. *ACS Appl. Mater. Inter.* 3 (7), 2585–2593.
- Yu, J., Chi, R., Zhang, Y., Xu, Z., Xiao, C., Guo, J., 2012. A situ co-precipitation method to prepare magnetic PMDA modified sugarcane bagasse and its application for competitive adsorption of methylene blue and basic magenta. *Bioresource Technol.* 110, 160–166.
- Zhang, S., Chao, Y., Zhang, C., Cheng, J., Li, J., Ma, N., Chen, S., Liu, X., 2010. Earthworms enhanced winter oilseed rape (*Brassica napus* L.) growth and nitrogen uptake. *Agr. Ecosyst. Environ.* 139 (4), 463–468.
- Zhou, Q., Gong, W., Xie, C., Yang, D., Ling, X., Yuan, X., Chen, S., Liu, X., 2011. Removal of Neutral Red from aqueous solution by adsorption on spent cottonseed hull substrate. *J. Hazard. Mater.* 185 (1), 502–506.